Title

Origins of Ca2+ Imaging with Fluorescent Indicators

Journal

Biochemistry, 60(46)

ISSN

0006-2960

Authors

Zhou, Xinqi
Belavek, Kayla J
Miller, Evan W

Publication Date

2021-11-23

DOI

10.1021/acs.biochem.1c00350

Peer reviewed

HHS Public Access

Author manuscript

Biochemistry. Author manuscript; available in PMC 2022 November 23.

Published in final edited form as:

Biochemistry. 2021 November 23; 60(46): 3547–3554. doi:10.1021/acs.biochem.1c00350.

Origins of Ca^{2+} imaging with fluorescent indicators

Xinqi Zhou[‡], **Kayla J. Belavek**[‡], **Evan W. Miller**[‡,§,†,*]

[‡]Department of Chemistry, University of California, Berkeley, California 94720, United States.

[§]Department of Molecular & Cell Biology, University of California, Berkeley, California 94720, United States.

[†]Department of Helen Wills Neuroscience Institute. University of California, Berkeley, California 94720, United States.

Abstract

In 1980, Roger Tsien published a paper, in this journal (*Biochemistry*, **1980**, *19* (11), 2396), describing "New calcium indicators and buffers with high selectivity against magnesium and protons: design, synthesis, and properties of prototype structures." These new buffers included 1,2-bis(o-aminophenoxy)ethane-*N,N,N',N'*-tetraacetic acid, or BAPTA, which remains in wide usage today. And so, the world was set alight with new ways in which to visualize Ca^{2+}. The ability to watch fluctuations in intracellular Ca^{2+} revolutionized the life sciences, although the fluorescent indicators used today, particularly neurobiology, no longer rely exclusively BAPTA but on genetically-encoded fluorescent Ca^{2+} indicators. In this Perspective, we reflect on the origins of Ca^{2+} imaging with a special focus on the contributions made by Roger Tsien, from the early concept of selective Ca^{2+} binding described in *Biochemistry*, to optical Ca^{2+} indicators based on chemically-synthesized fluorophores, through to genetically encoded fluorescent Ca^{2+} indicators.

Graphical Abstract

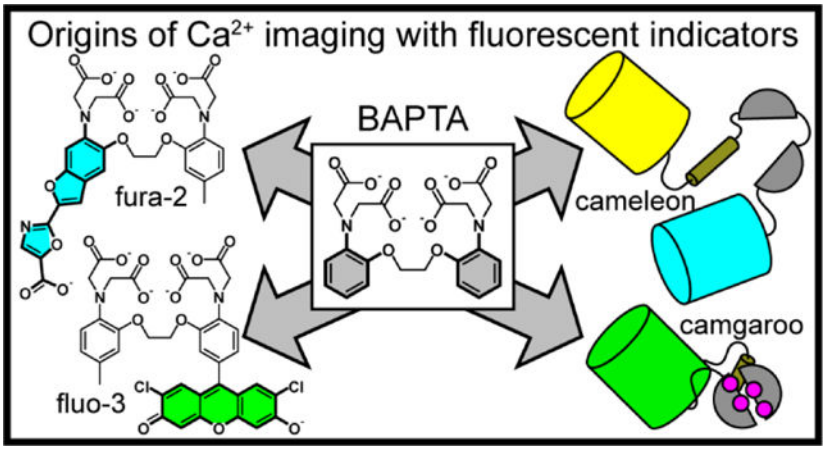

[*]Corresponding Author: evanwmiller@berkeley.edu.

Introduction

Ca^{2+} imaging in neurons is a mainstay of modern neurobiology. Using genetically encoded Ca^{2+} indicators (GECIs), combined with state-of-the-art optics and computational approaches, recording the activity of ensembles of neurons across large areas of the brains of model organisms is routine. From worms,[1] to flies,[2] to mice[3] and marmosets,[4] fluorescent Ca^{2+} indicators[5] have been deployed to paint a picture – or more fittingly, record a movie – of brain activity with cellular resolution. Together with advances in optogenetic approaches[6–8] – controlling neuronal activity with light – neurobiology has made substantial strides towards both measuring and manipulating brain activity with light.[9]

This Perspective aims to examine some of the origins of Ca^{2+} imaging. There have been many important contributions and contributors to this field. Inspired by a report published in 1980 by Roger Tsien in this journal,[10] we trace the involvement and influence of Roger Tsien on the field of Ca^{2+} imaging, starting with the development of BAPTA during his studies at Cambridge,[11] moving through synthetic Ca^{2+} indicators pioneered in his labs, and proceeding to the first variants of genetically encoded Ca^{2+} indicators. It is perhaps a fitting testament and tribute[11–14] to the prowess of the late Prof. Tsien that these innovations and their descendants are still in wide usage today.

BAPTA

Roger's initial paper describing BAPTA was a triumph of molecular design (Figure 1). The main Ca^{2+} chelator/buffer of the day, EGTA, solved the problem of achieving Ca^{2+}/Mg^{2+} selectivity (Mg^{2+} exists in a ~10,000:1 excess over cellular Ca^{2+}),[15] as Roger eloquently described in the original paper. The unique tetra carboxylate motif of EGTA could bind Ca^{2+} preferentially over Mg^{2+} because the larger ionic radius of Ca^{2+} allowed the carboxylates to form a perfectly-sized chelate. Mg^{2+}, on the other hand, with its smaller ionic radius, would force the anionic carboxylates into much closer proximity, inducing an energetic penalty for Mg^{2+} binding on account of charge repulsion.[10] However, the problem with EGTA was that binding of Ca^{2+} didn't induce a detectable optical change in the molecule. Furthermore, the aliphatic amines critical for binding Ca^{2+} were extremely basic: with pKa values of 9.0 and 8.6,[10] at physiological pH, the amines are primarily protonated. Not only did EGTA bind Ca^{2+} quite slowly, the binding kinetics were pH sensitive. Roger's simple, ingenious solution was to incorporate the aliphatic amine scaffold of EGTA into an aromatic framework, converting the alkyl amines into anilines (Figure 1). And thus, BAPTA was born.

BAPTA preserved the unique size and shape of EGTA which conferred its notable selectivity for Ca^{2+} over Mg^{2+}: BAPTA binds Ca^{2+} with a K_d of approximately 100 nM and binds Mg^{2+} with a K_d of approximately 20 mM.[10] The Ca^{2+} K_d of BAPTA (~100 nM) is well-matched to the Ca^{2+} K_d of EGTA (~150 nM, pH 7.2, 100 mM KCl).[16] This structural change also endowed BAPTA with a few critical improvements over EGTA. First, because the pKa of aniline nitrogens is several orders of magnitude lower than aliphatic amines (the two highest BAPTA pKa values are 6.4 and 5.5),[10] BAPTA binding of Ca^{2+} was no longer

pH dependent in the physiological range, and the binding kinetics of Ca^{2+} were improved compared to EGTA, allowing for reversible monitoring of both Ca^{2+} binding and release.[10]

However, and perhaps, more importantly, the aromatic rings of BAPTA now provided a visual cue that Ca^{2+} had bound to the BAPTA chelator. Upon complexation with Ca^{2+}, the lone pairs of electrons on the BAPTA nitrogens twist out of conjugation with the aromatic ring (Figure 1), shifting the absorbance band of BAPTA from “aniline-like” with a maximum of 254 nm in the absence of Ca^{2+} to one that was more “benzene-like”, with a maximum of 203 nm, when Ca^{2+} bound. The world now had an optical indicator that showed good selectivity for Ca^{2+} over Mg^{2+} ($>10^5$ selectivity) and H^+.

BAPTA had a few design limitations that precluded its use in living cells: 1) the absorbance of BAPTA was obscured by the more abundant protein and nucleic acids present in cells, which absorb in the same region of the spectrum, and 2) BAPTA is not fluorescent at visible wavelengths, making it unusable in cells. In addition to the wavelength problem, the other obstacle, at least to the application of BAPTA-based indicators to living cells, was that the structural motif essential for Ca^{2+} binding – the tetra carboxylic acids – rendered BAPTA-type chelators unable to cross cellular membranes. Roger would set out to solve both of these problems,[11] first in another sole-author paper[17] prior to starting his independent career at UC Berkeley, and second, in the unveiling of fura-2 in 1985.[16]

AM-esters

Roger realized that delivery of Ca^{2+} indicators to cells via microinjection would limit their wide-spread utility. So, he devised a method to chemically mask the tetra-carboxylate binding motif as an acetoxy-methyl ester (AM ester, Figure 2). The lipophilic tetra-ester crosses cell membranes, and ubiquitous cellular carboxy esterases remove the acetyl group, the resulting hemi-acetal decomposes to release an equivalent of methylene glycol (hydrated form of formaldehyde), and the exposed carboxylates can now bind Ca^{2+}. This method, inspired by pro-drug strategies used for antibiotics[18] remains the standard for delivery of synthetic Ca^{2+} indicators and other anionic small molecules to living cells. Recent innovations include bulky, hydrolytically stable AM esters for delivery to defined cells.[19]

Ratio-based Ca^{2+} imaging

The other challenge still facing those who wanted to visualize Ca^{2+} in living systems was the wavelength problem associated with BAPTA. Although BAPTA provided a visual cue that Ca^{2+} binding had taken place, the wavelengths were far too short (<254 nm) to be useful in cells. To address this, Roger built a chromophore around the BAPTA binding motif. A prototype of this strategy was presented alongside BAPTA in the 1980 *Biochemistry* paper. The quinoline-containing Ca^{2+} chelator (quin-2),[10] along with the recently developed AM esters, enabled bulk measurement of intracellular Ca^{2+} dynamics in intact lymphocytes.[20] The low brightness of quin-2 prompted the exploration of additional motifs for visualizing intracellular Ca^{2+}. In 1985, Roger reported the improved Ca^{2+} indicator fura-2, in which the BAPTA core was extended to include a benzofuran fluorophore (Figure 3).[16] Binding of Ca^{2+} induced the same conformational rotation of the aniline and shifted the absorbance

maximum of fura-2 by about 30 nm (Figure 3b). The emission wavelength was relatively unchanged as a result of Ca^{2+} binding, which allowed practitioners to switch excitation wavelengths to alternatively excite the Ca^{2+}-bound form (335 nm) or the Ca^{2+}-free form (362 nm) of fura-2 while monitoring same emission band, likely because Ca^{2+} dissociates from the amine in the excited state.[21]

By taking the ratio of the emission intensity in cells excited at the wavelengths corresponding to the Ca^{2+}-bound and -free forms of fura-2, one could estimate an actual Ca^{2+} concentration in living cells. The two excitation wavelengths allowed for correction of experimentally confounding factors like uneven loading of the dye in different cellular compartments or tissues, fluctuations in excitation source intensity, drifts in detector sensitivity or photo-bleaching. The bathochromic wavelength shift in fura-2 compared to BAPTA and quin-2 was far enough to push fura-2 into a range that could be used in living cells. Despite the requirement for UV excitation, which can be damaging to cells and tissue, fura-2 was received with open arms. It was widely adopted and remains the best and most widely-used ratio-based Ca^{2+} indicator, some 35 years after its initial report. The original paper has >21,000 citations according to Web of Science, and, in 2006 was the sixth most cited article in the history of the *Journal of Biological Chemistry*.[22] Another compound in the same article, indo-1, nicely complements fura-2, affording ratio-based imaging of Ca^{2+} via emission, and making it useful for flow cytometry[23] and confocal microscopy.[24]

Intensity-based Ca^{2+} imaging

Fura-2 combined several key intellectual developments to provide ratio-based optical estimations of intracellular Ca^{2+} concentration: the BAPTA chelator to achieve selectivity for Ca^{2+} over Mg^{2+} and H^+, AM esters to deliver optical indicators into living cells, and a benzofuran fusion with BAPTA to provide wavelengths that could be used in living cells. However, high energy UV excitation was prohibitive in some contexts. To expand into the visible wavelengths, Roger decoupled the BAPTA Ca^{2+}-sensing unit from the fluorescent reporter. Whereas in fura-2, BAPTA was incorporated into the benzofuran fluorophore, this next generation of Ca^{2+} indicators divorced the Ca^{2+} sensing motif (BAPTA) from the fluorescent reporter (which now had the freedom to be any fluorophore). The first two examples of this new strategy made use of fluorescein and rhodamine. To achieve Ca^{2+} sensing with these xanthene dyes, Roger connected BAPTA to the pendant aryl ring of the fluorescein or rhodamine, generating the Ca^{2+}-sensitive fluorophores christened fluo-1, −2, or −3 and rhod-1 or −2 (Figure 4).

These new indicators sense Ca^{2+} via a different mechanism from fura-2, a mechanism that involves photoinduced electron transfer, or PeT (Figure 5a). In the absence of Ca^{2+}, the electron-rich BAPTA short circuits fluorescence by donating, or transferring, an electron into the photoinduced excited state of the fluorescein or rhodamine. When BAPTA binds Ca^{2+}, this lowers the highest occupied molecular orbital (HOMO) of BAPTA, because the molecular orbitals of the xanthene fluorophore and the BAPTA chelating group are largely electronically decoupled because of the orthogonality of the fused xanthene ring system and the aryl ring at the 9’ position[25] (although the original intent of molecules like fluo-2

was to maintain some electronic coupling and induce a Ca^{2+}-dependent shift in absorbance, excitation, or emission wavelength)[26]

This lowers the free energy of PeT and makes the PeT process less efficient. As a result, binding Ca^{2+} increases fluorescence and the dye brightens (Figure 5b). Unlike fura-2, the Ca^{2+}-induced change in the optical properties of fluoand rhod-type dyes is an increase in the fluorescence quantum yield at a single wavelength, precluding estimates of actual Ca^{2+} concentration. However, fluo-2 and its progeny had the advantage of matching commonly available excitation and emission courses in microscopes world-wide, and the ability to track *changes* in Ca^{2+} levels, in real time, using commercially available microscopes was quickly adopted.

Second generation intensity-based Ca^{2+} indicators

As the Tsien lab increasingly turned its attention to the development of GFP, others continued the development of new variants of Ca^{2+} indicators (many of these efforts are reviewed more extensively elsewhere);[27–28] fluo-4, which used the recently developed 2',7'-fluorofluorescein,[29] is still in use to this day, as is Oregon Green BAPTA (OGB) which, while also using the fluorofluorescein developed at Molecular Probes, made use instead of an amide linkage to connect BAPTA to the fluorophore (Figure 4). This insulating attachment (rather than direct incorporation as in the fluo-X series), along with the presence of the 3-carboxylate on the aryl ring, gives OGB a higher fluorescence quantum yield than its corresponding fluo-X cousins.[27] Since these initial reports, there have been a profusion of intensity-based Ca^{2+} indicators (up to fluo-8, at the present), which largely use BAPTA, although with some modification to the substituent *para* to the BAPTA nitrogen, which allows tuning of BAPTA's affinity for Ca^{2+} across a wide swatch of useful concentration ranges, from nanomolar to low micromolar. Excellent reviews compiling wavelength, binding affinities, and usage guidelines for the wide array of chemically-synthesized Ca^{2+} indicators are available.[27–28]

Improving intensity- and ratio-based indicators

Ca^{2+} imaging at even longer wavelengths can be achieved with rhodamine fluorophores, such as X-Rhod-1 or Ca Ruby,[30] which contain a julolidine-derived[31] rhodamine 101[32] core (Figure 4). Development in xanthene dye chemistry has allowed access to orange, red, and far-red emitting fluorophores that possess the compact, three-ring structure of fluorescein and rhodamine. The groups at the fore-front of exploring these new chemistries applied the lessons of Roger Tsien's lab to generating new Ca^{2+} indicators that push Ca^{2+} sensing into new regions of the visible spectrum with indicators like Ca Tokyo Magenta (CaTM, Figure 4)[33–34] or Ca silicon rhodamine (CaSIR2, Figure 4).[35] Advances in rhodamine synthesis also allowed BAPTA to be positioned outside of the canonical 9' position on the xanthene dyes, resulting in Ca^{2+} indicators with improved brightness and response to Ca^{2+} (Compounds **1–5**, Figure 4).[36]

On the other hand, improvements and derivatives of fura-2 have been fewer. Fura-red (Figure 4) attempts to extend ratio-based imaging into the visible spectrum, but fura-

red[37] is quite dim and Ca^{2+} binding further lowers the fluorescence quantum yield.[38] Benzothiazolium-coumarin dyes like BTC (Figure 4) show red-shifted ratio-based responses to Ca^{2+}, but with binding affinities in the >7 μM range.[39] Other improvements include clever ways to anchor fura-2 (and derivatives) to macromolecules[40] or self-labeling enzymes[41] to improve cellular retention and localization.[42] But robust methods for ratio-based imaging with long wavelengths using a fura-type scaffold remain an outstanding challenge. In particular, the move to replace mercury arc lamps with light-emitting diodes (LEDs) means that the ability to perform ratio-based Ca^{2+} imaging in living cells is becoming the provenance of specialized microscopes: LEDs with excitation wavelengths at the 340/380 nm wavelengths for fura-2 are not common and require bespoke instrumentation.[43]

Alternative sensing modalities

Chemically-synthesized Ca^{2+} indicators afford the opportunity to extend to modalities beyond visible light. For example, magnetic resonance imaging (MRI) agents like DOPTA-Gd that change contrast in response to Ca^{2+} binding make use of BAPTA to achieve Ca^{2+}-sensitive MR contrast (Figure 4).[44–46] Synthetic efforts continue to push Ca^{2+} imaging into the near infrared region of the electromagnetic spectrum.[47–48] More recently, chemical-genetic hybrids have been employed, combining the Ca^{2+}-binding properties of genetically-encoded approaches[49–50] (see below) with modern fluorophores.[51–52]

Genetically encoded Ca^{2+} indicators (GECIs)

Delivery of chemically-synthesized Ca^{2+}-sensitive fluorophores, especially into tissues within intact organisms, remains a challenge. Although AM ester allow passage of fluorescent dyes across cellular membranes, their inclusion substantially decreases water solubility of the masked Ca^{2+} indicators. The advent of green fluorescent protein (GFP), and the optimized[53] and multi-color variants[54] developed in the Tsien lab, fundamentally altered this landscape. Today, the use of genetically-encoded Ca^{2+} indicators (GECIs) based off of GFP derivatives is ubiquitous across the field of neurobiology, especially for applications that involve *in vivo* imaging of neuronal activity.

Two-component indicators, or cameleons

The first example of a genetically encoded Ca^{2+}-sensitive indicator (GECI) shows not only the rapid advances that had been made since the first demonstration of heterologous expression of GFP in 1994,[55] but also the advances in creative nomenclature compared to synthetic indicators.

Cameleon was the first FP-based Ca^{2+} indicator to be expressed in cells and used to monitor Ca^{2+} dynamics (Figure 6a).[56] Cameleon used two variants of GFP, cyan fluorescent protein (CFP) and yellow fluorescent protein (YFP). CFP was fused to the N-terminus of calmodulin (CaM), a naturally-ocurring Ca^{2+}-binding protein, which was in turn connected to the N-terminus of the CaM-binding peptide, M13, fused to YFP. Because of the close proximity of the two FP fluorophores and the overlap of the emission spectra of CFP with the excitation spectra of YFP, excitation of CFP could induce emission from YFP

via radiationless dipole-dipole interactions known as Förster resonance energy transfer, or FRET.[58] Increases in Ca^{2+} levels results in the formation of a complex between CaM and Ca^{2+}, which can in turn bind to M13. Changes in the conformation of the intervening linker between CFP and YFP increases the FRET ratio. Practically speaking, the ratio of emission from YFP when exciting CFP (donor) to the emission from YFP (acceptor) when exciting it directly would reveal the extent of Ca^{2+} binding to CaM and the concentration of intracellular Ca^{2+}. Cameleon was so named because it changes color upon binding Ca^{2+} and extends a long tongue (M13) into and out of the mouth of calmodulin, which is abbreviated CaM.[56]

Similar to fura-2, cameleon and related FRET indicators can provide an estimate of intracellular Ca^{2+} concentrations by use of a ratio-based correction. Descendants of cameleons include indicators that use troponin C as a template for Ca^{2+} binding,[59] that use computationally-designed CaM-M13 pairs that are orthogonal to the native versions,[60] or use circularly permuted YFP.[61] However, it was the intensity-based indicators that eventually became more widely used in neurobiology for functional imaging in animal brains.

Single-component indicators, or camgaroo and GCaMP

Intensity-based genetically encoded Ca^{2+} indicators use a single FP to monitor changes in Ca^{2+} concentration. Here, too, Roger Tsien and co-workers showed the early way forward.[49] Circular permutants[62] of GFP, in which the N and C termini are migrated to different loops and regions of the FP and the original termini joined via a linker, place the FP chromophore closer to the solvent, breaking the protective “shell” formed by the β-barrel of GFP. Appending CaM/M13 at the ends of the new termini allowed conformational changes wrought by Ca^{2+} interactions with CaM and M13 to be effectively translated to the protein region surrounding the FP fluorophore, creating Ca^{2+}-dependent fluorescence. This type of configuration carried out with enhanced yellow fluorescent protein (EYFP) was christened camgaroo. A cheeky footnote in the original manuscript states that camgaroo is an “apt nickname” because “it is yellowish, carries a smaller companion (calmodulin = M13) inserted in its ‘pouch,’ can bounce high in signal, and may spawn improved progeny.”[49]

Camgaroo did indeed spawn more progeny. Both G-CaMP[50] and pericam[63] are circularly permuted GFPs or YFPs that use the same CaM/M13 strategy. Subsequent generations of G-CaMP (eventually shortened to GCaMP) have been used widely across model organisms, including fish, flies, worms, and mice.[3, 5] Multiple rounds of systematic mutagenesis led to generations of GCaMPs[5, 64] – all of which kept the cpGFP core and CaM/M13 binding partners – improving Ca^{2+} binding kinetics, increasing brightness, and enhancing the optical response to Ca^{2+} binding. The sixth generation, GCaMP6,[3] has become nearly ubiquitous in neurobiological imaging, owing, in part, to the ease of use, and the availability of indicators with tailored properties: fast variants (GCaMP6f), with fast Ca^{2+} binding and release kinetics, slower variants (GCaMP6s) with larger increases in fluorescence, but slower Ca^{2+} response and release kinectics.[3] Subsequent generations of GCaMP continue to improve brightness and reduce toxicity: jGCaMP7[65] was the first generation to include “j,” presumably to indicate the provenance of these discoveries, Janelia Research Campus.

Like synthetic Ca^{2+} indicators, GECIs have expanded into other wavelengths,[66–69] although the GFP-based indicators remain the most widely used.

Conclusions/Future Directions

Ca^{2+} imaging has a rich history and a bright future. Our goal in this Perspective was two-fold: to trace some of the origins of Ca^{2+} imaging to the seminal paper published in *Biochemistry*[10] and to highlight the contributions that one scientist in particular, Roger Tsien, made towards illuminating our understanding of neurobiology. Science, of course, is a team- and community-based endeavor, and our goal here is not to overlook the contributions made by others, but to highlight one scientist's involvement in so many facets of this journey.

In the future, inspired by the contributions over the last 40 years, we look forward to new innovations, with improved ratio-based imaging at long wavelengths, advanced microscopies for imaging deeper in the brain,[70–72] and less invasive methods for monitoring Ca^{2+} that do not rely on light alone.[71–72]

Acknowledgements

EWM acknowledges support from the Camille Dreyfus Teacher Scholar Fellows program and the NIH (R01NS098088). KJB was supported, in part, by a training grant from the NIH (T32GM066698).

REFERENCES

1. Larsch J; Ventimiglia D; Bargmann CI; Albrecht DR, High-throughput imaging of neuronal activity in *Caenorhabditis elegans*. Proceedings of the National Academy of Sciences 2013, 110 (45), E4266–E4273.
2. Seelig JD; Jayaraman V, Neural dynamics for landmark orientation and angular path integration. Nature 2015, 521 (7551), 186–191. [PubMed: 25971509]
3. Chen TW; Wardill TJ; Sun Y; Pulver SR; Renninger SL; Baohan A; Schreiter ER; Kerr RA; Orger MB; Jayaraman V; Looger LL; Svoboda K; Kim DS, Ultrasensitive fluorescent proteins for imaging neuronal activity. Nature 2013, 499 (7458), 295–300. [PubMed: 23868258]
4. Ebina T; Masamizu Y; Tanaka YR; Watakabe A; Hirakawa R; Hirayama Y; Hira R; Terada S-I; Koketsu D; Hikosaka K; Mizukami H; Nambu A; Sasaki E; Yamamori T; Matsuzaki M, Two-photon imaging of neuronal activity in motor cortex of marmosets during upper-limb movement tasks. Nature Communications 2018, 9 (1), 1879.
5. Tian L; Hires SA; Mao T; Huber D; Chiappe ME; Chalasani SH; Petreanu L; Akerboom J; McKinney SA; Schreiter ER; Bargmann CI; Jayaraman V; Svoboda K; Looger LL, Imaging neural activity in worms, flies and mice with improved GCaMP calcium indicators. Nature methods 2009, 6 (12), 875–81. [PubMed: 19898485]
6. Deisseroth K; Hegemann P, The form and function of channelrhodopsin. Science (New York, N.Y.) 2017, 357 (6356), eaan5544.
7. Hüll K; Morstein J; Trauner D, In Vivo Photopharmacology. Chemical Reviews 2018, 118 (21), 10710–10747. [PubMed: 29985590]
8. Tochitsky I; Kienzler MA; Isacoff E; Kramer RH, Restoring Vision to the Blind with Chemical Photoswitches. Chemical Reviews 2018, 118 (21), 10748–10773. [PubMed: 29874052]
9. Scanziani M; Häusser M, Electrophysiology in the age of light. Nature 2009, 461 (7266), 930–939. [PubMed: 19829373]

10. Tsien RY, New calcium indicators and buffers with high selectivity against magnesium and protons: design, synthesis, and properties of prototype structures. Biochemistry 1980, 19 (11), 2396–2404. [PubMed: 6770893]
11. Adams SR, Roger Y Tsien (1952–2016). Angewandte Chemie International Edition 2016, 55 (45), 13926–13927.
12. Kleinfeld D, Roger Tsien 1952–2016. Nature Neuroscience 2016, 19 (10), 1269–1270. [PubMed: 27669983]
13. Rink TJ; Tsien LY; Tsien RW, Roger Yonchien Tsien (1952–2016). Nature 2016, 538 (7624), 172–172. [PubMed: 27734865]
14. Palmer AE; Zhang J, Roger Y Tsien 1952–2016. Nature Chemical Biology 2016, 12 (11), 887–887. [PubMed: 27669418]
15. Romani AMP, Cellular magnesium homeostasis. Archives of Biochemistry and Biophysics 2011, 512 (1), 1–23. [PubMed: 21640700]
16. Grynkiewicz G; Poenie M; Tsien RY, A new generation of Ca2+ indicators with greatly improved fluorescence properties. Journal of Biological Chemistry 1985, 260 (6), 3440–3450.
17. Tsien RY, A non-disruptive technique for loading calcium buffers and indicators into cells. Nature 1981, 290 (5806), 527–8. [PubMed: 7219539]
18. Jansen ABA; Russell TJ, 379. Some novel penicillin derivatives. Journal of the Chemical Society (Resumed) 1965, (0), 2127–2132.
19. Tian L; Yang Y; Wysocki LM; Arnold AC; Hu A; Ravichandran B; Sternson SM; Looger LL; Lavis LD, Selective esterase–ester pair for targeting small molecules with cellular specificity. Proceedings of the National Academy of Sciences 2012, 109 (13), 4756–4761.
20. Tsien RY; Pozzan T; Rink TJ, Calcium homeostasis in intact lymphocytes: cytoplasmic free calcium monitored with a new, intracellularly trapped fluorescent indicator. Journal of Cell Biology 1982, 94 (2), 325–334.
21. Tsien RY, Calcium as a Cellular Regulator. Klee ECCB; Carafoli E; Klee CB, Eds. Oxford University Press: 1999; p 34.
22. Kresge N; Simoni RD; Hill RL, The Chemistry of Fluorescent Indicators: the Work of Roger Y. Tsien. Journal of Biological Chemistry 2006, 281 (37), e29–e31.
23. Rabinovitch PS; June CH; Grossmann A; Ledbetter JA, Heterogeneity among T cells in intracellular free calcium responses after mitogen stimulation with PHA or anti-CD3. Simultaneous use of indo-1 and immunofluorescence with flow cytometry. The Journal of Immunology 1986, 137 (3), 952–961. [PubMed: 2424993]
24. Tsien RY; Bacskai BJ, Video-Rate Confocal Microscopy. In Handbook of Biological Confocal Microscopy, Pawley JB, Ed. Springer US: Boston, MA, 1995; pp 459–478.
25. Urano Y; Kamiya M; Kanda K; Ueno T; Hirose K; Nagano T, Evolution of Fluorescein as a Platform for Finely Tunable Fluorescence Probes. Journal of the American Chemical Society 2005, 127 (13), 4888–4894. [PubMed: 15796553]
26. Minta A; Kao JPY; Tsien RY, Fluorescent indicators for cytosolic calcium based on rhodamine and fluorescein chromophores. Journal of Biological Chemistry 1989, 264 (14), 8171–8178.
27. Paredes RM; Etzler JC; Watts LT; Zheng W; Lechleiter JD, Chemical calcium indicators. Methods (San Diego, Calif.) 2008, 46 (3), 143–51.
28. Oheim M; van ‘t Hoff M; Feltz A; Zamaleeva A; Mallet J-M; Collot M, New red-fluorescent calcium indicators for optogenetics, photoactivation and multi-color imaging. Biochimica et Biophysica Acta (BBA) - Molecular Cell Research 2014, 1843 (10), 2284–2306. [PubMed: 24681159]
29. Sun W-C; Gee KR; Klaubert DH; Haugland RP, Synthesis of Fluorinated Fluoresceins. The Journal of Organic Chemistry 1997, 62 (19), 6469–6475.
30. Gaillard S; Yakovlev A; Luccardini C; Oheim M; Feltz A; Mallet J-M, Synthesis and Characterization of a New Red-Emitting Ca2+ Indicator, Calcium Ruby. Organic Letters 2007, 9 (14), 2629–2632. [PubMed: 17552530]
31. Titus JA; Haugland R; Sharrow SO; Segal DM, Texas Red, a hydrophilic, red-emitting fluorophore for use with fluorescein in dual parameter flow microfluorometric and fluorescence microscopic studies. Journal of immunological methods 1982, 50 (2), 193–204. [PubMed: 6806389]

32. Cooksey CJ, Quirks of dye nomenclature. 5. Rhodamines. Biotechnic & Histochemistry 2016, 91 (1), 71–76. [PubMed: 26529223]
33. Egawa T; Hirabayashi K; Koide Y; Kobayashi C; Takahashi N; Mineno T; Terai T; Ueno T; Komatsu T; Ikegaya Y; Matsuki N; Nagano T; Hanaoka K, Red Fluorescent Probe for Monitoring the Dynamics of Cytoplasmic Calcium Ions. Angewandte Chemie International Edition 2013, 52 (14), 3874–3877. [PubMed: 23440861]
34. Hirabayashi K; Hanaoka K; Egawa T; Kobayashi C; Takahashi S; Komatsu T; Ueno T; Terai T; Ikegaya Y; Nagano T; Urano Y, Development of practical red fluorescent probe for cytoplasmic calcium ions with greatly improved cell-membrane permeability. Cell Calcium 2016, 60 (4), 256–65. [PubMed: 27349490]
35. Numasawa K; Hanaoka K; Ikeno T; Echizen H; Ishikawa T; Morimoto M; Komatsu T; Ueno T; Ikegaya Y; Nagano T; Urano Y, A cytosolically localized far-red to near-infrared rhodamine-based fluorescent probe for calcium ions. Analyst 2020, 145 (23), 7736–7740. [PubMed: 33000768]
36. Deo C; Sheu S-H; Seo J; Clapham DE; Lavis LD, Isomeric Tuning Yields Bright and Targetable Red Ca2+ Indicators. Journal of the American Chemical Society 2019, 141 (35), 13734–13738. [PubMed: 31430138]
37. DeMarinis RM; Katerinopoulos HE; Muirhead KA New tetracarboxylate compounds as fluorescent intracellular calcium indicators. US4849362A, 1989.
38. Kurebayashi N; Harkins AB; Baylor SM, Use of fura red as an intracellular calcium indicator in frog skeletal muscle fibers. Biophysical journal 1993, 64 (6), 1934–60. [PubMed: 8369415]
39. Iatridou H; Foukaraki E; Kuhn MA; Marcus EM; Haugland RP; Katerinopoulos HE, The development of a new family of intracellular calcium probes. Cell Calcium 1994, 15 (2), 190–8. [PubMed: 8149419]
40. Konishi M; Watanabe M, Resting cytoplasmic free Ca2+ concentration in frog skeletal muscle measured with fura-2 conjugated to high molecular weight dextran. The Journal of general physiology 1995, 106 (6), 1123–50. [PubMed: 8786353]
41. Bannwarth M; Corrêa IR; Sztretye M; Pouvreau S; Fellay C; Aebischer A; Royer L; Ríos E; Johnsson K, Indo-1 Derivatives for Local Calcium Sensing. ACS Chemical Biology 2009, 4 (3), 179–190. [PubMed: 19193035]
42. Pendin D; Norante R; De Nadai A; Gherardi G; Vajente N; Basso E; Kaludercic N; Mammucari C; Paradisi C; Pozzan T; Mattarei A, A Synthetic Fluorescent Mitochondria-Targeted Sensor for Ratiometric Imaging of Calcium in Live Cells. Angewandte Chemie International Edition 2019, 58 (29), 9917–9922. [PubMed: 31132197]
43. Tinning PW; Franssen AJPM; Hridi SU; Bushell TJ; McConnell G, A 340/380 nm light-emitting diode illuminator for Fura-2 AM ratiometric Ca2+ imaging of live cells with better than 5 nM precision. Journal of Microscopy 2018, 269 (3), 212–220. [PubMed: 28837217]
44. Li W.-h.; Fraser SE; Meade TJ, A Calcium-Sensitive Magnetic Resonance Imaging Contrast Agent. Journal of the American Chemical Society 1999, 121 (6), 1413–1414.
45. MacRenaris KW; Ma Z; Krueger RL; Carney CE; Meade TJ, Cell-Permeable Esterase-Activated Ca(II)-Sensitive MRI Contrast Agent. Bioconjugate Chemistry 2016, 27 (2), 465–473. [PubMed: 26689452]
46. Adams CJ; Krueger R; Meade TJ, A Multimodal Ca(II) Responsive Near IR-MR Contrast Agent Exhibiting High Cellular Uptake. ACS Chemical Biology 2020, 15 (2), 334–341. [PubMed: 31967770]
47. Collot M; Ponsot F; Klymchenko AS, Ca-NIR: a ratiometric near-infrared calcium probe based on a dihydroxanthene-hemicyanine fluorophore. Chemical Communications 2017, 53 (45), 6117–6120. [PubMed: 28530289]
48. Ozmen B; Akkaya EU, Infrared fluorescence sensing of submicromolar calcium: pushing the limits of photoinduced electron transfer. Tetrahedron Letters 2000, 41 (47), 9185–9188.
49. Baird GS; Zacharias DA; Tsien RY, Circular permutation and receptor insertion within green fluorescent proteins. Proceedings of the National Academy of Sciences 1999, 96 (20), 11241–11246.
50. Nakai J; Ohkura M; Imoto K, A high signal-to-noise Ca(2+) probe composed of a single green fluorescent protein. Nature biotechnology 2001, 19 (2), 137–41.

51. Grimm JB; Muthusamy AK; Liang Y; Brown TA; Lemon WC; Patel R; Lu R; Macklin JJ; Keller PJ; Ji N; Lavis LD, A general method to fine-tune fluorophores for live-cell and in vivo imaging. Nature methods 2017, 14 (10), 987–994. [PubMed: 28869757]
52. Deo C; Abdelfattah AS; Bhargava HK; Berro AJ; Falco N; Farrants H; Moeyaert B; Chupanova M; Lavis LD; Schreiter ER, The HaloTag as a general scaffold for far-red tunable chemigenetic indicators. Nature Chemical Biology 2021.
53. Heim R; Prasher DC; Tsien RY, Wavelength mutations and posttranslational autoxidation of green fluorescent protein. Proceedings of the National Academy of Sciences 1994, 91 (26), 12501–12504.
54. Shaner NC; Campbell RE; Steinbach PA; Giepmans BN; Palmer AE; Tsien RY, Improved monomeric red, orange and yellow fluorescent proteins derived from Discosoma sp. red fluorescent protein. Nature biotechnology 2004, 22 (12), 1567–72.
55. Chalfie M; Tu Y; Euskirchen G; Ward WW; Prasher DC, Green Fluorescent Protein as a Marker for Gene Expression. Science (New York, N.Y.) 1994, 263 (5148), 802–805.
56. Miyawaki A; Llopis J; Heim R; McCaffery JM; Adams JA; Ikura M; Tsien RY, Fluorescent indicators for Ca2+based on green fluorescent proteins and calmodulin. Nature 1997, 388 (6645), 882–887. [PubMed: 9278050]
57. Romoser VA; Hinkle PM; Persechini A, Detection in living cells of Ca2+-dependent changes in the fluorescence emission of an indicator composed of two green fluorescent protein variants linked by a calmodulin-binding sequence. A new class of fluorescent indicators. The Journal of biological chemistry 1997, 272 (20), 13270–4. [PubMed: 9148946]
58. Lakowicz JR, Introduction to Fluorescence. In Principles of Fluorescence Spectroscopy, Lakowicz JR, Ed. Springer US: Boston, MA, 2006; pp 1–26.
59. Mank M; Santos AF; Direnberger S; Mrsic-Flogel TD; Hofer SB; Stein V; Hendel T; Reiff DF; Levelt C; Borst A; Bonhoeffer T; Hübener M; Griesbeck O, A genetically encoded calcium indicator for chronic in vivo two-photon imaging. Nature methods 2008, 5 (9), 805–11. [PubMed: 19160515]
60. Palmer AE; Giacomello M; Kortemme T; Hires SA; Lev-Ram V; Baker D; Tsien RY, Ca2+ indicators based on computationally redesigned calmodulin-peptide pairs. Chemistry & biology 2006, 13 (5), 521–30. [PubMed: 16720273]
61. Nagai T; Yamada S; Tominaga T; Ichikawa M; Miyawaki A, Expanded dynamic range of fluorescent indicators for Ca^{2+} by circularly permuted yellow fluorescent proteins. Proceedings of the National Academy of Sciences of the United States of America 2004, 101 (29), 10554–10559. [PubMed: 15247428]
62. Heinemann U; Hahn M, Circular permutation of polypeptide chains: implications for protein folding and stability. Progress in biophysics and molecular biology 1995, 64 (2–3), 121–43. [PubMed: 8987381]
63. Nagai T; Sawano A; Park ES; Miyawaki A, Circularly permuted green fluorescent proteins engineered to sense Ca^{2+}. Proceedings of the National Academy of Sciences 2001, 98 (6), 3197–3202.
64. Akerboom J; Chen T-W; Wardill TJ; Tian L; Marvin JS; Mutlu S; Calderón NC; Esposti F; Borghuis BG; Sun XR; Gordus A; Orger MB; Portugues R; Engert F; Macklin JJ; Filosa A; Aggarwal A; Kerr RA; Takagi R; Kracun S; Shigetomi E; Khakh BS; Baier H; Lagnado L; Wang SS-H; Bargmann CI; Kimmel BE; Jayaraman V; Svoboda K; Kim DS; Schreiter ER; Looger LL, Optimization of a GCaMP Calcium Indicator for Neural Activity Imaging. The Journal of Neuroscience 2012, 32 (40), 13819–13840. [PubMed: 23035093]
65. Dana H; Sun Y; Mohar B; Hulse BK; Kerlin AM; Hasseman JP; Tsegaye G; Tsang A; Wong A; Patel R; Macklin JJ; Chen Y; Konnerth A; Jayaraman V; Looger LL; Schreiter ER; Svoboda K; Kim DS, High-performance calcium sensors for imaging activity in neuronal populations and microcompartments. Nature methods 2019, 16 (7), 649–657. [PubMed: 31209382]
66. Zhao Y; Araki S; Wu J; Teramoto T; Chang YF; Nakano M; Abdelfattah AS; Fujiwara M; Ishihara T; Nagai T; Campbell RE, An expanded palette of genetically encoded Ca^{2+} indicators. Science (New York, N.Y.) 2011, 333 (6051), 1888–91.

67. Dana H; Mohar B; Sun Y; Narayan S; Gordus A; Hasseman JP; Tsegaye G; Holt GT; Hu A; Walpita D; Patel R; Macklin JJ; Bargmann CI; Ahrens MB; Schreiter ER; Jayaraman V; Looger LL; Svoboda K; Kim DS, Sensitive red protein calcium indicators for imaging neural activity. eLife 2016, 5.

68. Qian Y; Piatkevich KD; Mc Larney B; Abdelfattah AS; Mehta S; Murdock MH; Gottschalk S; Molina RS; Zhang W; Chen Y; Wu J; Drobizhev M; Hughes TE; Zhang J; Schreiter ER; Shoham S; Razansky D; Boyden ES; Campbell RE, A genetically encoded near-infrared fluorescent calcium ion indicator. Nature methods 2019, 16 (2), 171–174. [PubMed: 30664778]

69. Shemetov AA; Monakhov MV; Zhang Q; Canton-Josh JE; Kumar M; Chen M; Matlashov ME; Li X; Yang W; Nie L; Shcherbakova DM; Kozorovitskiy Y; Yao J; Ji N; Verkhusha VV, A near-infrared genetically encoded calcium indicator for in vivo imaging. Nature biotechnology 2021, 39 (3), 368–377.

70. Ouzounov DG; Wang T; Wang M; Feng DD; Horton NG; Cruz-Hernández JC; Cheng YT; Reimer J; Tolias AS; Nishimura N; Xu C, In vivo three-photon imaging of activity of GCaMP6-labeled neurons deep in intact mouse brain. Nature methods 2017, 14 (4), 388–390. [PubMed: 28218900]

71. Lakshmanan A; Jin Z; Nety SP; Sawyer DP; Lee-Gosselin A; Malounda D; Swift MB; Maresca D; Shapiro MG, Acoustic biosensors for ultrasound imaging of enzyme activity. Nature Chemical Biology 2020, 16 (9), 988–996. [PubMed: 32661379]

72. Rabut C; Yoo S; Hurt RC; Jin Z; Li H; Guo H; Ling B; Shapiro MG, Ultrasound Technologies for Imaging and Modulating Neural Activity. Neuron 2020, 108 (1), 93–110. [PubMed: 33058769]

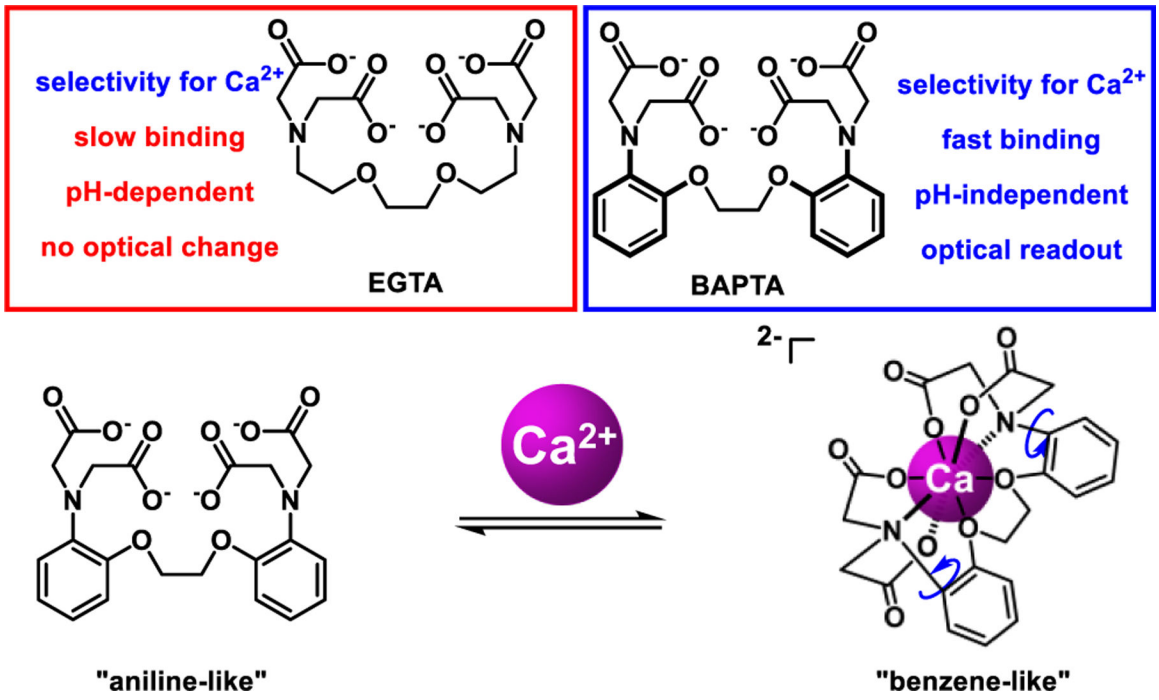

Figure 1.

Structures of EGTA and BAPTA. Annulation of EGTA results in BAPTA, which retains the overall shape of EGTA (conferring Ca^{2+} selectivity over Mg^{2+}), but with less basic aniline nitrogens, which lowers the pH sensitivity and improves binding kinetics of BAPTA. Binding of Ca^{2+} results in a shift from an “aniline-like” structure to a “benzene-like” structure.

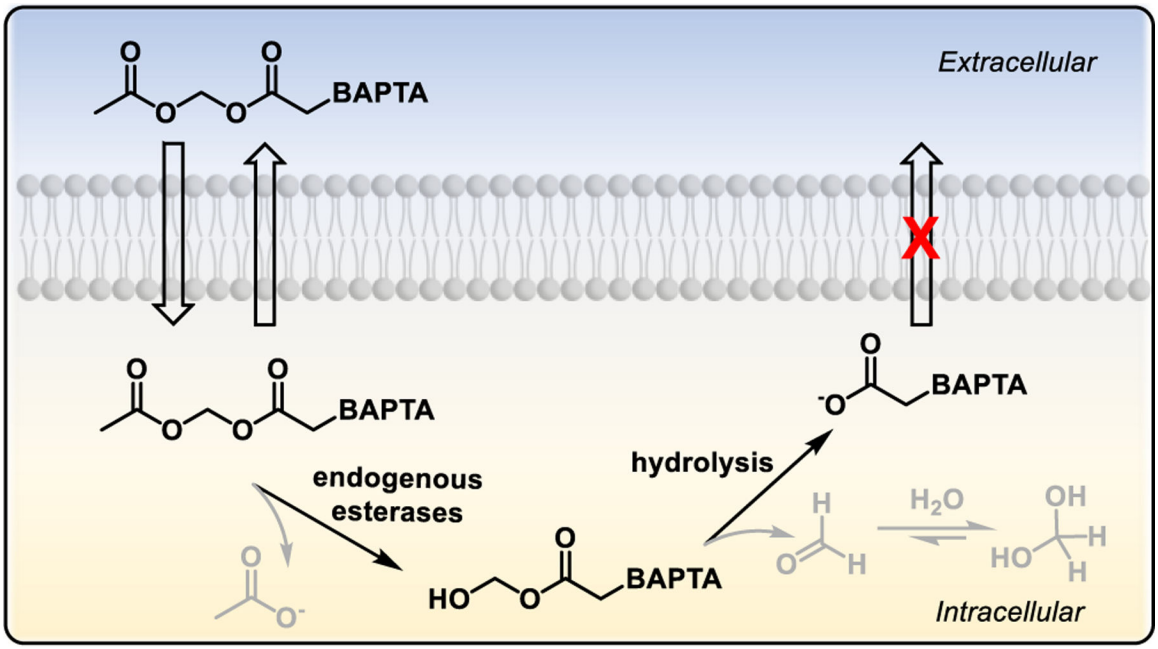

Figure 2.
Delivery of small molecules to cells via acetoxymethyl (AM) esters.

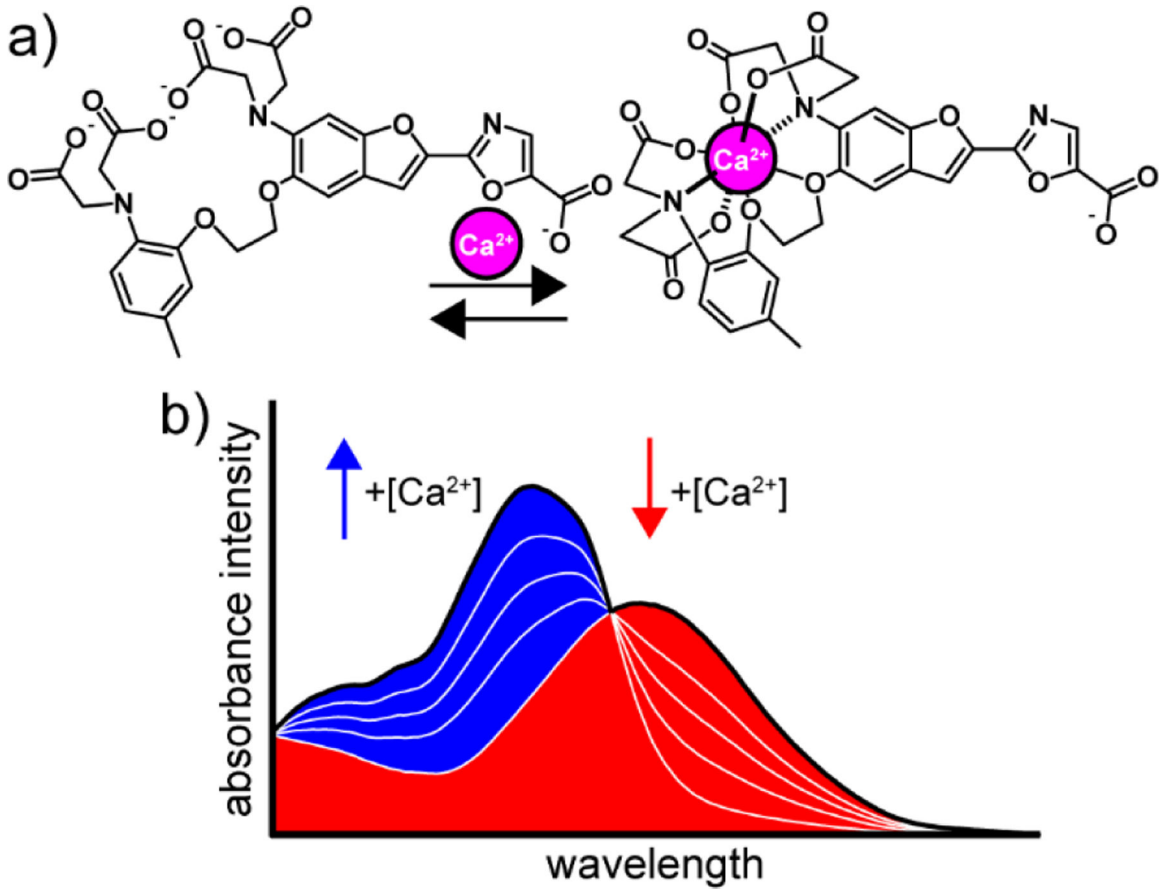

Figure 3.

Fura-2 structure and Ca^{2+} binding. **a)** Structures of the Ca^{2+}-free and Ca^{2+}-bound fura-2. **b)** Binding of Ca^{2+}results in a blue-shift of fura-2 absorbance, with little change in the emission wavelength.

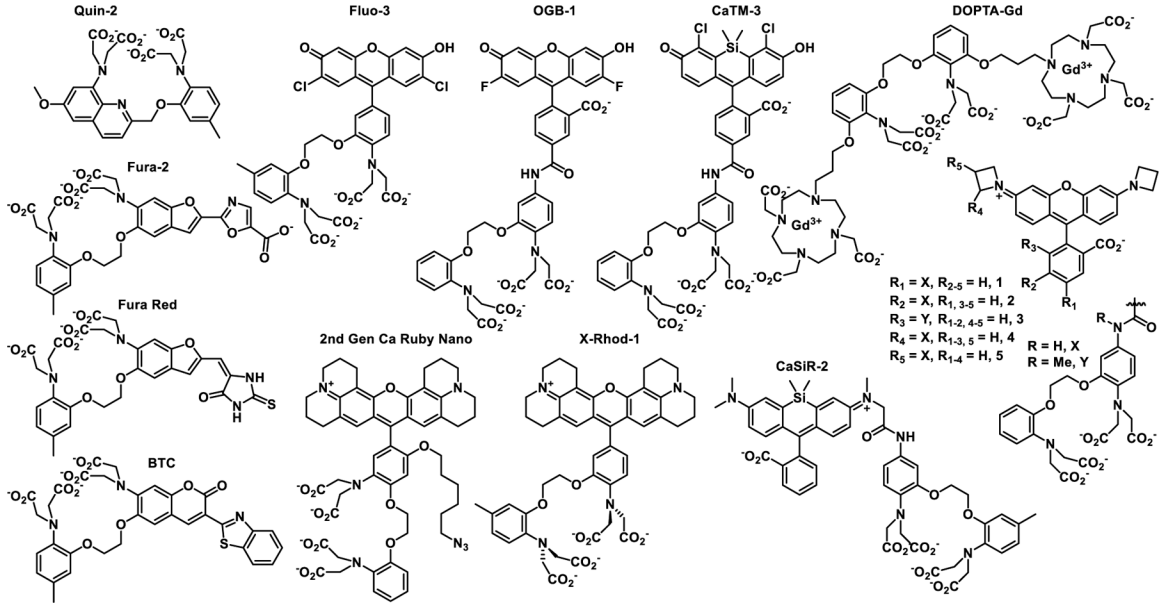

Figure 4.

Structures of synthetic Ca^{2+} indicators. Quin-2, Fura-2, and Fluor-3 are all first generation indicators developed by Tsien and co-workers. Fura-2, Fura Red, and BTC are ratio-based indicators. Fluo-3, OGB-1, CaTM-3, Ca Ruby Nano, X-Rhod, CaSiR-2, and Compounds **1**–**5** are all intensity-based indicators.

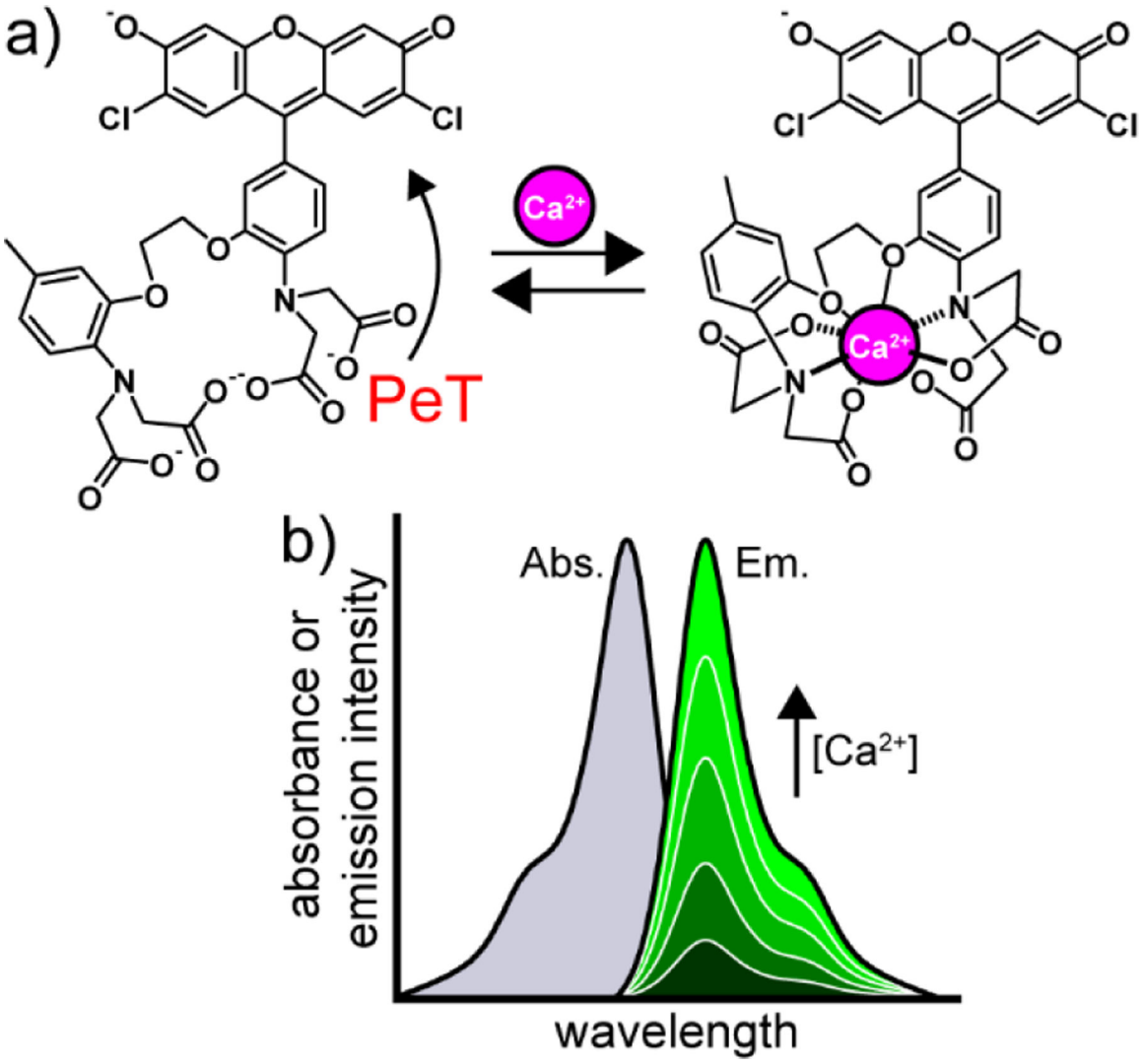

Figure 5.

Fluo-3 structure and mechanism. **a)** Structure and binding of fluo-3 to Ca^{2+}. In the absence of Ca^{2+}, photoinduced electron transfer (PeT) from the electron-rich BAPTA group quenches fluorescence. Binding of Ca^{2+} relieves PeT, and the dye becomes more fluorescent. **b)** Representative plot of fluo-3 absorbance (grey) and emission (green) vs. wavelength with increasing Ca^{2+} concentration. Although emission intensity increases upon addition of Ca^{2+}, the absorbance spectra of fluo-3 remains relatively unchanged.

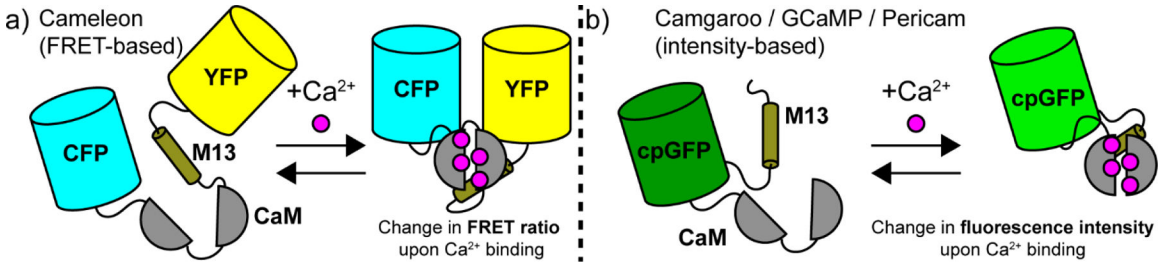

Figure 6.

Genetically encoded Ca^{2+} indicators of **a)** "cameleon" or **b)** "camgaroo" lineages. Cameleon-style indicators use two fluorescent proteins to alter FRET efficiency upon Ca^{2+} binding. Camgaroo-style indicators use a single fluorescent protein (cpGFP, or GCaMP, is shown in this figure).